

DIFFERENTIAL LOCALIZATION OF GABA_A RECEPTOR SUBUNITS IN RELATION TO RAT STRIATO-PALLIDAL AND PALLIDO-PALLIDAL SYNAPSES. A. Gross^{1,2}, R.E. Sims¹, J.D. Swinny³, W. Sieghart⁴, J.P. Bolam², I.M. Stanford¹

¹ Aston University, School of Life and Health Sciences, Birmingham, U.K.;

² MRC Anatomical Neuropharmacology Unit, Dept of Pharmacology, Oxford, U.K.;

³ University of Portsmouth, School of Pharmacy and Biomedical Sciences, Portsmouth, U.K.;

⁴ Medical University of Vienna, Vienna, Austria.

Abbreviated title: GABA_A receptor subunits in the GP

Key words: Globus Pallidus, immunofluorescence, zolpidem

Number of pages:	35
Number of figures:	7
Number of tables	1
Number of words (Abstract):	245
Number of words (Introduction):	496
Number of words (Total)	9698

Correspondence should be addressed to;

Ian M. Stanford
Aston University,
The School of Life and Health Sciences,
Birmingham. B4 7ET, U.K.
Tel - 0121 204 4015
E-mail I.M.Stanford@aston.ac.uk

ABSTRACT

As a central integrator of basal ganglia function, the external segment of the globus pallidus (GP) plays a critical role in the control of voluntary movement. The GP is composed of a network of inhibitory GABA containing projection neurons which receive GABAergic input from striatum (Str) axons and local collaterals of GP neurons. Here, using electrophysiological techniques and immunofluorescent labeling we have investigated the differential cellular distribution of $\alpha 1$, $\alpha 2$, $\alpha 3$ GABA_A receptor subunits in relation to striato-pallidal (Str-GP) and pallido-pallidal (GP-GP) synapses.

Electrophysiological investigations showed that zolpidem (100 nM - selective for the $\alpha 1$ subunit) increased the amplitude and the decay time of both Str-GP and GP-GP IPSCs, indicating the presence of the $\alpha 1$ subunits at both synapses. However, the application of drugs selective for the $\alpha 2$, $\alpha 3$ and $\alpha 5$ subunits (zolpidem at 400 nM, L-838,417 and TP003), revealed differential effects on amplitude and decay time of IPSCs suggesting the non-uniform distribution of non- $\alpha 1$ subunits.

Immunofluorescence revealed widespread distribution of the $\alpha 1$ subunit at both soma and dendrites, while double- and triple-immunofluorescent labeling for parvalbumin, enkephalin, gephyrin and the $\gamma 2$ subunit, indicated strong immunoreactivity for GABA_A $\alpha 3$ subunits in perisomatic synapses, a region mainly targeted by local axon collaterals. In contrast, immunoreactivity for synaptic GABA_A $\alpha 2$ subunits was observed in dendritic compartments where striatal synapses are preferentially located. Due to the kinetic properties which each GABA_A α subunits confer, this distribution is likely to differentially contribute to both physiological and pathological patterns of activity.

INTRODUCTION

The basal ganglia (BG) consist of a group of nuclei involved in a variety of functions, including motor control, and are the principal site of pathology in a variety of diseases including Parkinson's disease. Driven by intrinsic mechanisms and excitatory glutamatergic inputs from the subthalamic nucleus (STN), neurons of the globus pallidus (GP, external segment of the globus pallidus in primates) process and transmit information from the striatum to the STN (Smith et al., 1990; Parent & Hazrati, 1995), the internal segment of the globus pallidus (Kincaid et al., 1991), the substantia nigra pars reticulata (Smith & Bolam, 1989) and the striatum (Bevan et al., 1998). Neurons of the GP are thus in a position to powerfully influence activity of the whole BG (Bolam et al., 2000).

The GP is composed of a network of inhibitory GABAergic projection neurons. Ninety percent of their afferent synapses are GABAergic, arising from the striatum and the axon collaterals of neighbouring GP neurons. The GP boutons preferentially innervate the soma and proximal dendrites of GP neurons (Kita & Kitai, 1994; Sato et al., 2000) in the form of peri-neuronal nets (Shink et al., 1996; Sadek et al., 2007). Electrophysiological studies (Sims et al., 2008) have revealed significant differences in the characteristics of striato-pallidal (Str-GP) and pallido-pallidal (GP-GP) synapses which may be due to differential expression of GABA_A subunits.

GABA_A receptors are hetero-pentameric channels composed of a family of receptor subunits. Functional GABA_A receptors require the co-assembly of 2 α , 2 β and one other subunit (Barnard, 1995; Tretter et al., 1997; Farrar et al., 1999), the most common form being composed of 2 α , 2 β , 1 γ (Ernst et al., 2003; Benke et al., 2004). Different subunits confer different pharmacological and electrophysiological properties (Sieghart, 1995). Thus, receptors containing the α 1 subunit have fast deactivation and desensitization kinetics (Freund & Buzsaki, 1996; Klausberger et al., 2002), whereas those containing the α 2 subunit

show rapid activation but slow deactivation rates (Lavoie et al., 1997), and an apparent ten-fold higher affinity for GABA (Levitan et al., 1988). The β subunit appears to be an integral part of the recognition site for GABA (Amin & Weiss, 1993) and has a role in receptor desensitization (Newell & Dunn, 2002) while the γ subunit, together with the α subunit, is associated with the benzodiazepine-binding site (Sieghart, 1995; Sigel, 2002; Ernst et al., 2003) and is implicated in clustering at synaptic sites through interaction with the microtubule protein gephyrin (Ramming et al., 2000; Fritschy et al., 2008).

Previous reports indicate dense immunoreactivity for GABA_A α 1, β 2, γ 1 subunits and weaker immunoreactivity for GABA_A α 2, α 3, β 3 and γ 2 subunits (Fritschy et al., 1992; Fritschy & Mohler, 1995; Pirker et al., 2000; Schwarzer et al., 2001) in the GP. In this study, our aim was to determine whether different GABA_A receptor subunits are selectively associated with Str-GP and GP-GP synapses and thus underlie differences in the properties of the synapses. This was done by a combination of electrophysiological, pharmacological and immunofluorescence analyses.

MATERIALS AND METHODS

All the animals in this study were used in accordance with the Animals (Scientific Procedures) Act, 1986 (UK) and in accordance with the European Community Council Directive of 24th November 1986 (86/609/EEC).

Electrophysiology

18-22 day old male Wistar rats used in this study were bred from a colony originally obtained from Charles River (Kent, U.K.). Rats were first anaesthetized with isoflurane in 2% O₂ until cardio-respiratory arrest and then decapitated. Brain slices (300 µm) were then cut on a DTK-1000 Microslicer (Dosaka, Japan) in a sucrose-based solution comprising (mM): sucrose, 206; KCl, 2.5; CaCl₂·2H₂O, 1; NaHCO₃, 26; NaH₂PO₄, 1.25; MgCl₂·6H₂O, 2; glucose, 10; indomethacin, 0.045. The slices were then incubated at room temperature for 1 h in artificial cerebrospinal fluid (aCSF) comprising (in mM): NaCl, 126; KCl, 2.5; CaCl₂·2H₂O, 2; NaHCO₃, 26; NaH₂PO₄, 1.2; MgCl₂·6H₂O, 1.3; glucose, 10. Cutting solution and aCSF were equilibrated with 95%:5% O₂:CO₂, pH 7.4. Slices were then transferred to a recording chamber perfused with aCSF at a rate of 2 ml/min, at 32°C. Neurons were visualized by differential interference contrast infrared microscopy using with an Olympus BX51W1 microscope together with a CCD KP-M1 camera (Hitachi, Japan).

Whole-cell patch-clamp recordings were made using borosilicate glass pipettes (1.5-2.5 MΩ resistance) and filled with a chloride-based internal solution, comprising (mM); KCl, 125; NaCl, 10; CaCl₂, 1; MgCl₂, 2; HEPES, 10; GTP, 0.3; Mg-ATP, 2; BAPTA, 10 (adjusted to pH 7.3 with KOH).

Membrane currents were recorded in neurons voltage-clamped at -80 mV using an Axopatch 700A patch-clamp amplifier (Molecular Devices, U.S.A.). Series resistance (3-20 MΩ) was monitored throughout experiments and compensated > 60%. Results from neurons

where series resistance changed over 20% throughout the analysis, or was greater than 20 M Ω , were discarded.

Focal stimulation was applied with glass electrodes filled with aCSF, and carried out using a DS-3 isolated stimulator (Digitimer, U.K.) with pulses of 0.1 ms width and 0.02-1 mA at 0.2 Hz. To block NMDA and AMPA receptors that may have been activated by glutamatergic inputs from the STN or possibly the pedunculopontine nucleus, 50 μ M 2-AP5 and 10 μ M CNQX was routinely added to the aCSF. Selective stimulation of Str-GP synapses and GP-GP synapses was achieved as described previously (Sims et al., 2008). In brief, for the stimulation of Str-GP connections, sagittal sections were used and electrodes were placed in dense axonal bundles within the striatum itself. For the stimulation of GP-GP connections, coronal sections were used, thus reducing the impact of Str-GP inputs. In these experiments stimulating electrodes were placed in the GP itself, away from striato-pallidal axonal bundles but within 200 μ m of the recorded GP neuron.

The use of sagittal and coronal sections to separate Str-GP inputs from GP-GP inputs is based upon the knowledge that Str-GP projections project along the rostro-caudal axis (Wilson & Phelan, 1982) and that the dendritic arbour of many GP neurons lies perpendicular to this striatal input (Kita & Kitai, 1994). These planes of section have been used previously to separate Str-GP inputs from GP-GP inputs and show differential sensitivity to dopamine D2 agonists (Cooper & Stanford, 2000) and Str-GP sensitivity to cannabinoid CB1 agonists (Engler et al., 2006).

Striatal inputs are therefore effectively negated in slices cut in the coronal plane, allowing stimulation of GP-GP inputs without extensive contamination. However, cross-stimulation is still a possibility as up to 30% of GP neurons project back to the striatum (Bevan et al., 1998). Thus, there was the potential that striatal stimulation antidromically activate GP axons which would contaminate presumed Str-GP responses. Antidromic responses were occasionally

observed but were easily identified as the amplitude was directly proportional stimulation intensity and peaked within 0.1ms of the stimulation artefact. All data showing evidence of antidromic activity were discarded. We acknowledge that antidromic stimulation of other GP cells may take place, which may then release GABA onto our recorded cell. However, the precise location and stimulation strength was manipulated to evoke IPSCs without failures and without multiple peaks which may arise through stimulation multiple fibres and/or the activation of polysynaptic networks.

Data were recorded at 10 kHz, and filtered by an 8-pole low-pass Bessel filter at 4 kHz using a Multiclamp 700A amplifier, and digitized by a Digidata 1322A. Analysis was performed online with Clampex 9.2 and offline using Clampfit 9.2 (all Molecular Devices, USA). The amplitude of each IPSC was measured from a point immediately before the stimulation artefact while decay times were calculated by fitting single exponential curves in Clampfit 9.2. In the data traces presented, stimulation artefacts were removed offline. All data is expressed as mean \pm standard error mean, unless otherwise stated. The Mann-Whitney U-test was used to assess differences from baseline recordings 15 minutes after drug application and $P < 0.05$ was considered significant.

Drugs

2-AP5 and CNQX were supplied by Ascent Scientific (U.K.), diazepam (non-selective benzodiazepine) from Sigma UK and zolpidem (selective for the GABA_A α 1 subunit) and L-838,417 (selective efficacy for GABA_A α 2, α 3 and α 5 subunits) from Tocris (U.K.). TP003 (GABA_A α 3 subunit selective agonist) was supplied by and used with the permission of Merck Research Laboratories (New Jersey, USA). All drugs were initially made in 1000x stock solutions and diluted to the final concentration in aCSF immediately prior to application.

Immunofluorescent labeling

Immunofluorescent localization of GABA_A receptor subunits can often yield false negative or unspecific labeling as some of these proteins are sensitive to the aldehyde concentrations used in fixation process. Therefore, we optimised our fixation protocol to reach the most ideal labeling, using 1% paraformaldehyde and low pH fixation for the $\alpha 3$ experiments, and 2% paraformaldehyde in combination with pepsin digestion for all the other immunoreactions.

Six adult Sprague-Dawley rats (250-450 g; Charles River, Margate, U.K.) were used. Each animal was anesthetized with phenobarbital, and perfused with approximately 50 ml of phosphate buffered saline (PBS; 0.01 M phosphate buffer, pH 7.4, 0.876% NaCl, 0.02% KCl) via the ascending aorta, followed by about 200 ml of fixative (0.1 M phosphate buffer, pH 7.4, 1 or 2% paraformaldehyde, 15% saturated picric acid) over a period of 25 min. For the GABA_A $\alpha 3$ subunit experiments the fixative consisted of 1% paraformaldehyde in Na-acetate buffer at pH 6. Free fixative was removed by post-perfusion with PBS. The brains were removed and 60 μ m sagittal sections cut using a vibrating blade microtome (VT1000S; Leica).

Sections for most of the immunoreactions (except the reactions with the $\alpha 3$ antibody, where no pepsin treatment was used) were washed in 0.1 M phosphate buffer (PB), and then treated with 0.02% pepsin (P-7125, Sigma-Aldrich Chemie, Steinheim, Germany) to unmask the antigens and epitopes thus enhancing staining intensity. Sections were pre-incubated for 2 h at room temperature in blocking solution, consisting of 20% normal donkey serum, 0.2% Triton X-100 in Tris buffered saline (TBS; 50 mM, pH 7.5, 0.9% NaCl). This was followed by overnight incubation at 4 °C with one or mixtures of primary antibodies against: GABA_A subunits ($\alpha 1$, $\alpha 2$, $\alpha 3$, $\gamma 2$), gephyrin, parvalbumin, enkephalin, vesicular GABA transporter (VGAT) and anti-human neuronal protein (anti-HuC/D).

Details of origin, specificity and dilutions of antibodies are described in Table 1. Sections were then washed and incubated in mixture of fluorescent tagged secondary antibodies.

Finally, sections were washed, mounted and cover-slipped using fluorescence mounting medium (Vectashield, Vector Laboratories, Inc., Burlingame, CA, U.S.A.).

Controls

The specificity of GABA_A α 1, α 2, α 3 and γ 2 antibodies have all been previously tested in knock-out animals (see Table 1 for references). To test for cross-reactivity between various antibodies sections were processed with a full complement of secondary antibodies and one primary antibody at a time. None of the combinations with species-unrelated secondary antibodies resulted in labeling. In addition, no selective labeling was found in sections incubated with combinations of secondary antibodies without a primary antibody (see supplementary Table).

Imaging and data acquisition

Images were captured with a LSM 710 (Zeiss, Göttingen Germany) confocal microscope with; Plan-Apochromat 63x/1.40 oil and 40x/1.3 or 20x objectives. For low magnification LSM images 10x objective was used. The ZEN 2008 software's default settings for the fluorophors were used for beam splitters and ranges of emissions sampled. **Two channel z-stacks were acquired using the SRS automatic acquisition function, following a manual pre-focussing step at all capture sites, and projection images were analyzed. However, for a better quality, single images are presented in the figures.** For stereological analysis, three sections from two animals were analyzed using a fluorescence capable Stereo- Investigator system (MBF Biosciences, MicroBrightField Europe, Magdeburg, Germany). The boundary of the GP was drawn at low (10x objective) magnification. A sampling grid was randomly positioned over the GP contour. The sizes of grids were chosen according to the abundance of analyzed neurons (240 x 180 μ m for α 1-HuC/D and 375 x 270 μ m for α 1-

gephyrin experiments). A counting frame of 125 x 90 μm was located at the top left of each grid cell.

RESULTS

IPSCs were evoked either by stimulation within the GP in coronal slices selectively activating GP-GP synapses or by stimulation in the striatum in sagittal slices selectively activating Str-GP synapses. Previous studies (Sims et al., 2008) have revealed differences in the kinetics of these evoked IPSCs and this was confirmed in the current experiments. Thus, rise times, decay times and half widths of Str-GP responses were significantly slower than GP-GP synapses, data which is consistent with local collaterals innervating the soma and proximal dendrites of GP neurons and striatal inputs preferentially innervating more distal regions.

In the first series of experiments the non-subunit selective benzodiazepine, diazepam was used. Diazepam (500 nM) increased the Str-GP evoked IPSC amplitude ($130.7 \pm 10.3\%$, $n = 6$, $P = 0.0006$, Mann-Whitney U-test) and GP-GP evoked IPSC amplitude ($141.3 \pm 15.4\%$, $n = 6$, $P = 0.0012$, Mann-Whitney U-test) after 15 min application (Fig. 1A/1-A/2). As expected from a benzodiazepine-mediated action, the decay time of the Str-GP and GP-GP evoked responses also significantly increased ($129.0 \pm 5.5\%$, $n=6$, $P = 0.0006$ and $132.4 \pm 8.9\%$, $n=6$, $P = 0.0012$, Mann-Whitney U-test) respectively (Fig. 1A/3-A/4).

In order to probe for the presence of GABA_A α 1-subunit density at Str-GP and GP-GP synapses, zolpidem was used at 100 nM, a concentration at which it shows selectivity for the α 1 subunit. At this concentration, zolpidem increased the Str-GP evoked IPSC amplitude ($141.1 \pm 13.7\%$, $n = 6$, $P = 0.0012$, Mann-Whitney U-test) and the GP-GP evoked IPSC amplitude ($147.0 \pm 12.3\%$, $n=6$, $P = 0.0012$, Mann-Whitney U-test) after 15 min application (Fig. 1B/1-B/2). The decay time of the Str-GP and GP-GP evoked responses also increased ($137.7 \pm 12.5\%$, $n=6$, $P = 0.0221$ and $140.7 \pm 8.0\%$, $n=6$, $P = 0.0012$, Mann-Whitney U-test) of baseline respectively (Fig. 1B/3-B/4). These data suggest that GABA_A receptors containing the α 1 subunit are located at both Str-GP and GP-GP synapses.

To complement the pharmacological data, we analyzed the cellular distribution of the GABA_A α 1 subunit. Strong immunoreactivity for the GABA_A α 1 subunit was detected throughout the GP (Fig. 2A). In order to determine the proportion of GP neurons that express the GABA_A α 1-subunit, double-labeling for the α 1-subunit with the neuronal marker HuC/D was carried out and the numbers of single- and double-labeled neurons counted in a sample of 3 sections from 2 animals. From these counts, we estimate that 80.6% (710 of a total number 881 neurons counted) of the total population of GP neurons express GABA_A α 1 subunit whereas the expression of the subunit was not detected in 19.4%.

GP neurons can be characterized based on the expression of the calcium binding protein, parvalbumin. Therefore, to determine whether the receptor subunits are expressed in parvalbumin-negative or parvalbumin-positive GP neurons, we performed triple-labeling experiments for GABA_A α 1, gephyrin and parvalbumin (Fig. 2B-E). We found that GABA_A α 1 subunit was co-localized with gephyrin and equally distributed on the soma (Fig. 2E, double arrowheads) and on dendrites of parvalbumin-positive and negative GP neurons (Fig. 2E, arrowheads).

We acknowledge that the co-localization of gephyrin with the α 1 subunit does not necessarily provide direct evidence for the synaptic location of the receptor subunit, since previous studies have reported both gephyrin-dependent and gephyrin-independent clustering of synaptic GABA_A α 1 subunit containing receptors (Kneussel et al., 2001, Levi et al., 2004). Indeed, this correlates with the observation that the population of GABA_A α 1-positive neurons expressed variable levels of gephyrin immunoreactivity within the soma. One group displayed only slightly stronger immunolabeling over background (Fig. 2C asterisk), whereas the immunolabeling of the other group was considerably higher than background (Fig. 2E arrows). This finding raises the question, whether neurons expressing low levels of gephyrin receive less inhibitory input, or express some other postsynaptic clustering protein.

To address this question triple labeling immunofluorescent experiments were performed with GABA_Aα1, gephyrin and VGAT. Qualitative analysis revealed that in both the weak and strong gephyrin-immunoreactive neurons, immunoreactivity for GABA_A α1 (Supp. Figure 1A) subunit and VGAT (Supp. Figure 1C) was equally strong (Supp. Figure 1D). Thus, both weakly and strongly gephyrin-immunoreactive GP neurons may equally be targeted by putative GABAergic terminals, suggesting that weakly gephyrin-positive GP neurons express some other protein besides gephyrin as a postsynaptic clustering protein.

Quantitative analysis of the GABA_A α1-gephyrin double-labeling experiments revealed that 76 % of α1-positive neurons in the GP are strongly positive for gephyrin (104 out of a total number of 136 neurons counted in 3 sections from 2 animals), as opposed to the remaining 24%, which are weakly positive for the synaptic marker (32 out of a total number 136 neurons counted in 3 sections from 2 animals) (Fig. 2F). Interestingly, those neurons that showed strong immunoreactivity for gephyrin were also positive for parvalbumin (Fig. 2E, arrows), whereas neurons showing low levels of gephyrin immunoreactivity appeared to be parvalbumin-negative (Fig. 2E, asterisk).

In addition to double labeling for gephyrin and GABA_A α1, we performed further double labeling experiments with antibodies against GABA_A γ2 subunit, which has also been shown to be required for postsynaptic clustering (Essrich et al., 1998). These experiments revealed the co-location of the GABA_A α1 subunits with the GABA_A γ2 subunit at both somatic and dendritic locations (Fig. 2K-M), similar to what we found with gephyrin.

Additionally, we determined whether we could detect any preferential localization of the GABA_A α1 subunit associated with striatal afferent terminals. In order to identify striatal terminals targeting GP neurons, we performed double labeling experiments with enkephalin antibodies. Taking into account that a small proportion of GP neurons have been shown to express preproenkephalin, a precursor for enkephalin (Voorn et al., 1999; Hoover and

Marshall 2002), it is still reasonable to suggest that the majority of the very dense enkephalin-immunoreactive terminals that are observed in GP are derived from the striatum (Fig. 2H). In all examined GABA_A α1 subunit-expressing neurons enkephalin immunoreactivity appeared to be distributed equally with somata and dendrites (Fig. 2G-J and 2J/1-4). This suggests that GABA_A α1 subunit is equally associated with striatal and GP synapse, which is consistent with the electrophysiological data (see above).

At 100 nM, zolpidem is considered to be selective for GABA_A receptors containing the α1 subunit whilst 400 nM zolpidem is considered non-selective, having significant efficacy also at GABA_A α2 and α3 subunit-containing receptors (Langer S.Z, 1992). In order to probe for the presence of GABA_A receptors containing non-α1 subunits at Str-GP and GP-GP synapses, IPSC amplitude and decay time were monitored whilst raising the concentration of zolpidem from 100 nM to 400 nM (Fig 3). This change in concentration had no effect on the amplitude of Str-GP IPSCs ($94.4 \pm 5.8\%$, $n=8$, $P = 0.7308$, Mann-Whitney U-test, Fig. 3A/1), but increased GP-GP IPSC amplitude ($112.6 \pm 3.7\%$, $n=8$, $P = 0.0012$, Mann-Whitney U-test, Fig. 3A/2) after 15 min application. However, the decay time of the evoked Str-GP and GP-GP IPSCs both increased to $111.4 \pm 3.0\%$ ($n=8$, $P = 0.0023$, Fig. 3A/3) and $118.6 \pm 5.4\%$ ($n=8$, $P = 0.0047$, Mann-Whitney U-test, Fig. 3A/4) respectively. The greater effect on GP-GP IPSCs of raising zolpidem concentration to 400nM, suggests that there is a higher density of non-α1 subunits at GP-GP synapses. To further test these data, experiments were carried out with L-838,417, an anxiolytic non-benzodiazepine compound that has no efficacy at GABA_A α1 subunits but acts as a partial agonist at α2, α3 and α5 subunits (McKernan et al., 2000). L-838,417 (500nM) had little effect on the amplitude of Str-GP IPSCs ($104.5 \pm 11.3\%$, $n=6$, $P = 0.4452$, Mann-Whitney U-test, Fig. 3B/1) or decay time ($103.6 \pm 5.7\%$, $n=6$, $P = 0.6282$, Mann-Whitney U-test, Fig. 3B/3), but significantly increased the amplitude ($129.3 \pm 12.1\%$,

$n=7$, $P = 0.0262$, Mann-Whitney U-test, Fig. 3B/2) and decay time ($125.2 \pm 5.1\%$, $n=7$, $P = 0.0005$, Mann-Whitney U-test Fig. 3B/4) of GP-GP IPSCs.

To assess which non- $\alpha 1$ subunit is responsible for the enhancement of the amplitude and decay time at GP-GP synapses (Fig. 3), immunofluorescent labeling for the GABA_A $\alpha 2$ subunit was carried out. Weak-to-moderate immunoreactivity for GABA_A $\alpha 2$ was found throughout the GP (Fig. 4A). The majority of GABA_A $\alpha 2$ -positive neurons examined were once again positive for parvalbumin (Fig. 4D, E). Although immunoreactivity for GABA_A $\alpha 2$ subunit was found in both somatic and dendritic compartments of individual GP neurons (Fig. 4B, E/1), a clearly stronger immunoreactivity for the GABA_A $\alpha 2$ subunit was observed in the dendrites (Fig. 4E/1, F).

Double immunofluorescent labeling for GABA_A $\alpha 2$ subunit and gephyrin revealed well-defined co-localization in dendritic compartments whereas co-localization was less pronounced at the soma. This suggests relatively more synaptic GABA_A $\alpha 2$ subunits in the dendrites of GP neurons (Fig. 4E-H).

The observation that the GABA_A $\alpha 2$ subunit appears preferentially located in dendritic compartments raises the question which subunit is responsible for the increased GP-GP responses observed in the presence of 400 nM zolpidem and L-838,417? As zolpidem has been reported to be ineffective at GABA_A $\alpha 5$ subunit-containing receptors (Pritchett & Seeburg, 1990; Langer S.Z, 1992) the most likely candidate is the GABA_A $\alpha 3$ subunit. In order to test this possibility, immunofluorescent labeling for GABA_A $\alpha 3$ subunit was carried out in combination with immunolabeling for $\alpha 1$ and $\gamma 2$ subunits, enkephalin, parvalbumin and HuC/D (Fig. 5A-D). Weak-to-moderate immunoreactivity for GABA_A $\alpha 3$ subunits was observed throughout the GP (Fig. 5A). The immunoreactivity for this subunit appeared to be both intracellular and membrane associated. In contrast to the $\alpha 2$ subunit immunoreactivity, the $\alpha 3$ subunit appeared to be more pronounced at the soma than in dendritic compartments (Fig.

5B, E, H, and L). Once again, gephyrin showed strong immunoreactivity throughout GP (Fig. 5F), whereas double-labeling with GABA_A α3 was mainly observed at the soma (Fig. 5G). Dense immunoreactivity for enkephalin was observed throughout the somato-dendritic axis of GP neurons (Fig 5I); immunoreactivity which was clearly associated with GABA_A α3 subunit-positive and parvalbumin-positive neurons (Fig. 5K). Although immunoreactivity for the synaptic marker GABA_A γ2 subunit was found at both somatic and dendritic locations, co-localization with the GABA_A α3 subunit was mainly observed at the soma (Fig 5L-N). As GP-GP synapses form peri-neuronal nets on the soma and proximal dendrites of GP cells (Shink et al., 1996; Sadek et al., 2007) it is expected that the GABA_A receptors, containing the α3 subunit are preferentially targeted by local axon collaterals arising from other GP neurons.

To test for the presence of GABA_A α3 subunits at GP-GP synapses we used the non-benzodiazepine TP003 (100 nM) which has significant selectivity at receptors containing α3 subunits (Dias et al., 2005). After 15 min application of 100 nM TP003, IPSCs evoked in sagittal slices by stimulation of the striatum showed no significant change in amplitude ($97.5 \pm 4.8\%$ $n=7$, $P = 0.0973$, Mann-Whitney U-test, Fig. 6A/1) or decay time ($102.9 \pm 5.8\%$, $n=7$, $P = 0.0973$, Mann-Whitney U-test, Fig. 6A/2). In contrast, IPSCs evoked in coronal slices by stimulation of GP showed significantly enhanced amplitude ($125.0 \pm 10.1\%$, $n=7$, $P = 0.0023$, Mann-Whitney U-test, Fig. 6B/1) without significant change in decay time ($108.7 \pm 5.9\%$, $n=7$, $P = 0.0734$, Mann-Whitney U-test Fig. 6B/2). These data provide further evidence for a role of the α3 subunit at GP-GP synapses.

DISCUSSION

Neurons of the GP receive inhibitory GABAergic input from the striatum and also from neighbouring neurons. Although not as dense as the striatal input, GP-GP synapses mainly innervate the soma and proximal dendrites where they form synapses in a peri-somatic basket-like pattern (Kita & Kitai, 1994; Sadek et al., 2007). In this study we have used this feature to correlate the properties of somatic GP-GP synapses and widespread Str-GP synapses with specific GABA_A α subunits.

Using zolpidem at a low concentration we have shown GABA_A α 1 subunit to be present in both GP-GP and Str-GP synapses. Furthermore, immunocytochemical data reveals a widespread distribution of the GABA_A α 1 subunit being present in both dendritic and somatic compartments. It is likely that the majority of GABA_A α 1 subunits are located within the synapse as they co-localize with the synaptic markers gephyrin and the GABA_A γ 2 subunit. In contrast, the GABA_A α 2 and α 3 subunits show a differential subcellular distribution. The α 2 subunit appeared to be preferentially located at distal dendritic compartments, where it is co-localized with gephyrin, whereas immunoreactivity for GABA_A α 3 subunit was confined to perisomatic regions where it co-localized with gephyrin and the γ 2 subunit. Unfortunately quantification of immunofluorescent puncta in GP was not possible due to the relatively poor labeling observed. This problem is most likely due to the anatomical properties of GP itself as simultaneous experiments using cortical and hippocampal tissue provided convincing, punctate labeling with both the GABA_A α 2 and α 3 antibodies. Quantification of these subunits was also attempted at ultra-structural level using electron microscopic analysis; however, once again poor labeling limited our analysis. Therefore, we were restricted to a qualitative light microscopic analysis complemented by the pharmacological and electrophysiological data.

Cellular distribution

In brain slice preparations, medium spiny projection neurons of the striatum display hyperpolarized resting membrane potentials commonly around -90mV and are therefore quiescent (Jiang & North, 1991). In contrast, the majority of GP neurons exhibit spontaneous activity (Nambu & Llinas, 1994; Cooper & Stanford, 2000). Based on the assumption that Str-GP inputs are more numerous, we initially thought that analysis of spontaneous action potential-driven IPSCs (arising from GP) and miniature IPSCs (the majority of which are presumed to be Str-GP in origin), should separate GP-GP and Str-GP activity. However, no kinetic differences between spontaneous or miniature IPSCS were observed leaving little confidence in the use of this type of analysis in the separation of these inputs. However, significant differences in the kinetics of evoked IPSCs were observed in coronal and sagittal slices indicating a better separation of GP-GP and Str-GP IPSCs. Thus, a typical GP-GP IPSC exhibits fast rise time, rapid decay and short half width while IPSCs elicited by Str-GP synapses are kinetically slower and significantly different from GP-GP IPSCs (Sims et al. 2008).

In order to differentiate between α -subunits pharmacologically, we initially used the hypnotic drug, zolpidem at 100 nM and 400 nM. When tested on recombinant receptors, zolpidem displays a high affinity at α 1-containing GABA_A receptors (α 1 β 2 γ 2, α 1 β 3 γ 2: K_i =20 nM), medium affinity at α 2- and α 3-containing GABA_A receptors (e.g. α 2 β 1 γ 2, α 3 β 1 γ 2: K_i =400 nM) and was ineffective at α 5 subunit-containing receptors (α 5 β 3 γ 2, α 5 β 2 γ 2: K_i 5000 nM, (Pritchett & Seeburg, 1990; Langer S.Z, 1992). Furthermore, with regard to potency, an approximate 5 to 8 fold higher zolpidem concentration was required to generate a comparable enhancement of GABA-induced chloride flux in α 2 β 3 γ 2 or α 3 β 3 γ 2 receptors (see Ramerstorfer et al., 2010 and references therein). We therefore maintain the concentrations of 100 nM and 400 nM zolpidem are good choices in order to differentiate between α 1 and

$\alpha 2/\alpha 3$ subunit containing receptors. This is further evidenced by the work of Crestani and colleagues (2000) who showed unequivocally, using mutated $\alpha 1$ subunits, that zolpidem acted as a sedative exclusively through $\alpha 1$ -subunit containing GABA_A receptors.

The GABA_A $\gamma 2$ subunit also appears critical for the activity of zolpidem (Cope et al., 2004). Previously it has been reported that GABA_A $\gamma 2$ subunits are only present in the dendrites of GP neurons (Schwarzer et al., 2001). Furthermore, enkephalin-positive medium spiny striatal neurons have been reported to exclusively innervate the dendritic shafts of GP neurons (Falls et al., 1983; Okoyama et al., 1987). This gave rise to the notion that striatal derived afferents preferentially innervate the dendrites of GP neurons and contain GABA_A $\gamma 2$ subunits. However, the data presented here indicates that GABA_A $\gamma 2$ subunits, as well as enkephalin-positive striatal axons and terminals, are more uniformly distributed over the whole GP neuronal architecture being present at both somatic and dendritic compartments.

Using zolpidem at a concentration of 100 nM we have shown GABA_A receptors containing the $\alpha 1$ subunit are located at both Str-GP and GP-GP synapses. Increasing zolpidem to a non-selective concentration (400 nM), caused an increase in amplitude of GP-GP but not Str-GP IPSCs, suggesting a larger proportion of non- $\alpha 1$ subunits at GP-GP synapses; a finding supported by the observations using the GABA_A $\alpha 3$ selective drug TP003. Thus, both GABA_A $\alpha 1$ and $\alpha 3$ subunit-containing receptors were preferentially found in the soma and regions of proximal dendrites where they would be selectively targeted by axon collaterals of other GP neurons (see Fig. 7). This also raises the possibility of localization of $\alpha 1$ alone or in combination with $\alpha 3$ (see Fig. 5D) (Benke et al., 2004).

Subcellular distribution of α -subunits.

Using double immunolabeling we have demonstrated the co-localization of GABA_A $\alpha 1$ $\alpha 2$ and $\alpha 3$ subunits with the GABA_A $\gamma 2$ subunit and gephyrin, which we used as a potential

marker for synaptic sites, thus indicating the synaptic localization of these α subunits. However, a significant proportion of the receptor subunits did not co-localize with gephyrin or the $\gamma 2$ subunit, possibly indicating that some subunits may be located extrasynaptically. Another possible explanation is that some GABA_A receptor subunits may not require gephyrin for postsynaptic clustering. However the precise nature of these GABA_A receptors remains unclear. It is currently accepted that the γ subunit is required for postsynaptic clustering, while the δ subunit confers extrasynaptic location when coupled to the $\alpha 4$ or $\alpha 6$ subunit (Nusser et al., 1998). The activation of extrasynaptic receptors give rise to tonic, background inhibitory conductance which can alter the input resistance of the neuron and influence synaptic efficacy and integration (Farrant & Nusser, 2005). However, there have been no reports indicating the presence of the δ subunit or indeed the presence of tonic inhibitory conductance in the GP. If a tonic conductance is present in GP, the results presented here would indicate that $\alpha 1$, $\gamma 2$ zolpidem-sensitive receptors may be involved (Semyanov et al., 2003).

Functional Implications.

The activation of GABA_A receptors provides inhibition on the millisecond time-scale and has therefore been implicated in regulating the temporal dynamics of neural networks (Cobb et al., 1995; Traub et al., 1996; Mann & Paulsen, 2007; Yamawaki et al., 2008), both in physiological and pathological states. With regard to the basal ganglia and the Parkinsonian, dopamine-depleted state, exaggerated oscillatory activity in the GP amongst other nuclei, is invariably found at a frequency in the β range (~ 20 Hz), which is implicated in the loss of ability to perform discrete movements in both Parkinson's disease patients (Brown & Marsden, 1998; Levy et al., 2000; Kuhn et al., 2006) and animal models of Parkinson's disease (Mallet et al., 2008). Indeed, GABA_A receptor-mediated IPSPs in the STN and GP appear to not only

provide tonic inhibition of downstream nuclei but also have a role in determining the timing of subsequent action potential firing by producing rebound spikes and phase realignment of the intrinsic subthreshold membrane oscillations (Bevan et al., 2002; Stanford, 2003; Rav-Acha et al., 2005).

It is widely accepted that peri-somatic inhibition primarily controls timing of activity and ultimately the regulation of overall neuronal output (Cobb et al., 1995; Miles et al., 1996; Freund & Katona, 2007). Moreover peri-somatic inhibition usually involves larger synaptic terminals, more synaptic vesicles and mitochondria, and larger active zones inducing IPSPs with faster kinetics and greater amplitude than those induced by dendrite-targeting interneurons (Miles et al., 1996). This is certainly the case in the GP where peri-neuronal nets of GP-GP terminals activate receptors containing $\alpha 1$ and $\alpha 3$ subunits on soma and proximal dendrites which would be expected to determine direct on/off signalling of activity. This finding also correlates with the peri-somatic innervation by terminals of other PV-positive GP neurons which constitute around 70% of the whole GP neuronal population (Kita, 1994). It remains to be determined how neuronal heterogeneity within the GP increases the complexity of the proposed schema. In contrast, dendritic inhibition may control the shunting and therefore efficacy of excitatory synaptic inputs or synaptic plasticity perhaps through the modulation of dendritic calcium spikes (Miles et al., 1996). In the hippocampus, parvalbumin-negative synapses showed five times more immunoreactivity for the GABA_A $\alpha 2$ subunit than synapses made by parvalbumin-positive basket cells (Nyiri et al., 2001; Klausberger et al., 2002). This rule appears to hold in the GP, where $\alpha 2$ subunit containing receptors are preferentially located at synapses targeting distal dendrites in regions where parvalbumin-positive input would be restricted.

In conclusion, our data suggest that the synapses formed by inhibitory terminals arising from the striatum and local axon collaterals from GP neurons, and target distinct neuronal

compartments are associated with different complement of GABA_A receptor subunits. These data add to the growing literature that each input will mediate different physiological functions.

ACKNOWLEDGMENTS

This work was supported by The Medical Research Council UK, Grant G0300179. Many thanks to Prof. Jean-Marc Fritschy for the gift of antibodies, Ben Micklem for his help with the imaging and stereology, Liz Norman, Katie Withworth and Caroline Francis for technical assistance and to Prof. P. Somogyi for helpful discussions.

ABBREVIATIONS

BG	- basal ganglia
GP	- globus pallidus
IPSC	- inhibitory postsynaptic current
STN	- subthalamic nucleus
Str	- striatum

REFERENCES

- Amin, J. & Weiss D.S. (1993) GABAA receptor needs two homologous domains of the beta-subunit for activation by GABA but not by pentobarbital. *Nature* **366**, 565-569.
- Barnard, E.A. (1995) The molecular biology of GABAA receptors and their structural determinants. *Adv. Biochem. Psychopharmacol.* **48**, 1-16.
- Benke, D., Fakitsas, P., Roggenmoser, C., Michel, C., Rudolph, U., Mohler, H. (2004) Analysis of the presence and abundance of GABAA receptors containing two different types of alpha subunits in murine brain using point-mutated alpha subunits. *J. Biol. Chem.* **279**, 43654-43660.
- Bevan, M.D., Booth, P.A., Eaton, S.A., Bolam, JP. (1998) Selective innervation of neostriatal interneurons by a subclass of neuron in the globus pallidus of the rat. *J. Neurosci.* **18**, 9438-9452.
- Bevan, M.D., Magill, P.J., Hallworth, N.E., Bolam, JP, Wilson, C.J. (2002) Regulation of the timing and pattern of action potential generation in rat subthalamic neurons in vitro by GABA-A IPSPs. *J. Neurophysiol.* **87**, 1348-1362.
- Bolam, JP, Hanley, J.J., Booth, P.A., Bevan, M.D. (2000) Synaptic organisation of the basal ganglia. *J. Anat.* **196** (Pt 4), 527-542.
- Brown, P. & Marsden, C.D. (1998) What do the basal ganglia do? *Lancet* **351**, 1801-1804.
- Cobb, S.R., Buhl, E.H., Halasy, K., Paulsen, O., Somogyi, P. (1995) Synchronization of neuronal activity in hippocampus by individual GABAergic interneurons. *Nature* **378**, 75-78.
- Cooper, A.J. & Stanford, I.M. (2000) Electrophysiological and morphological characteristics of three subtypes of rat globus pallidus neurone in vitro. *J. Physiol.* **527**, 291-304.
- Cope, D.W., Wulff, P., Oberto, A., Aller, M.I., Capogna, M., Ferraguti, F., Halbsguth, C., Hoeger, H., Jolin, H.E., Jones, A., McKenzie, A.N., Ogris, W., Poeltl, A., Sinkkonen, S.T., Vekovischeva, O.Y., Korpi, E.R., Sieghart, W., Sigel, E., Somogyi, P., Wisden, W. (2004) Abolition of zolpidem sensitivity in mice with a point mutation in the GABAA receptor gamma2 subunit. *Neuropharmacology* **47**, 17-34.
- Dias, R., Sheppard, W.F., Fradley, R.L., Garrett, E.M., Stanley, J.L., Tye, S.J., Goodacre, S., Lincoln, R.J., Cook, S.M., Conley, R., Hallett, D., Humphries, A.C., Thompson, S.A., Wafford, K.A., Street, L.J., Castro, J.L., Whiting, P.J., Rosahl, T.W., Atack, J.R., McKernan, R.M., Dawson, G.R., Reynolds, D.S. (2005) Evidence for a significant role of alpha 3-containing GABAA receptors in mediating the anxiolytic effects of benzodiazepines. *J. Neurosci.* **25**, 10682-10688.
- Engler, B., Freiman, I., Urbanski, M., Szabo, B. (2006) Effects of exogenous and endogenous cannabinoids on GABAergic neurotransmission between the caudate-putamen and the globus pallidus in the mouse. *J. Pharmacol. Exp. Ther.* **316**, 608-617.

- Ernst, M., Brauchart, D., Boesch, S., Sieghart, W. (2003) Comparative modeling of GABA(A) receptors: limits, insights, future developments. *Neuroscience* **119**, 933-943.
- Essrich, C., Lorez, M., Benson, J.A., Fritschy, J.M., Luscher, B. (1998) Postsynaptic clustering of major GABAA receptor subtypes requires the gamma 2 subunit and gephyrin. *Nat. Neurosci.* **1**, 563-571.
- Falls, W.M., Park, M.R., Kitai, S.T. (1983) An intracellular HRP study of the rat globus pallidus. II. Fine structural characteristics and synaptic connections of medially located large GP neurons. *J. Comp. Neurol.* **221**, 229-245.
- Farrant, M. & Nusser, Z. (2005) Variations on an inhibitory theme: phasic and tonic activation of GABA(A) receptors. *Nat. Rev. Neurosci.* **6**, 215-229.
- Farrar, S.J., Whiting, P.J., Bonnert, T.P., McKernan, R.M. (1999) Stoichiometry of a ligand-gated ion channel determined by fluorescence energy transfer. *J. Biol. Chem.* **274**, 10100-10104.
- Fornaro, M. & Geuna, S. (2005) Confocal imaging of HuC/D RNA-binding proteins in adult rat primary sensory neurons. *Annals of Anatomy* **183**, 471-473.
- Freund, T.F. & Buzsaki, G. (1996) Interneurons of the hippocampus. *Hippocampus* **6**, 347-470.
- Freund, T.F. & Katona, I. (2007) Perisomatic inhibition. *Neuron* **56**, 33-42.
- Fritschy, J.M. & Mohler, H. (1995) GABAA-receptor heterogeneity in the adult rat brain: differential regional and cellular distribution of seven major subunits. *J. Comp. Neurol.* **359**, 154-194.
- Fritschy, J.M., Harvey R.J., Schwarz, G. (2008) Gephyrin: where do we stand, where do we go? *Trends Neurosci.* **31**, 257-264.
- Fritschy, J.M., Benke, D., Mertens, S., Oertel, W.H., Bachi, T., Mohler, H. (1992) Five subtypes of type A gamma-aminobutyric acid receptors identified in neurons by double and triple immunofluorescence staining with subunit-specific antibodies. *Proc. Natl. Acad. Sci. USA* **89**, 6726-6730.
- Gronborg, M., Pavlos, N.J., Brunk, I., Chua, J.J., Munster-Wandowski, A., Riedel, D., Ahnert-Hilger, G., Urlaub, H., Jahn, R. (2010) Quantitative comparison of glutamatergic and GABAergic synaptic vesicles unveils selectivity for few proteins including MAL2, a novel synaptic vesicle protein. *J. Neurosci.* **30**, 2-12.
- Hoover, B.R. & Marshall, J.F. (2002) Further characterization of preproenkephalin mRNA-containing cells in the rodent globus pallidus. *Neuroscience* **111**, 111-25.
- Jacob, T.C., Bogdanov, Y.D., Magnus, C., Saliba, R.S., Kittler, J.T., Haydon, P.G., Moss, S.J. (2005) Gephyrin regulates the cell surface dynamics of synaptic GABAA receptors. *J. Neurosci.* **25**, 10469-10478.

- Jiang, Z.G. & North, R.A. (1991) Membrane properties and synaptic responses of rat striatal neurones in vitro. *J. Physiol.* **443**, 533-553.
- Kincaid, A.E., Penney, J.B. Jr., Young, A.B., Newman, S.W. (1991) Evidence for a projection from the globus pallidus to the entopeduncular nucleus in the rat. *Neurosci. Lett.* **128**, 121-125.
- Kita, H. (1994) Parvalbumin-immunopositive neurons in rat globus pallidus: a light and electron microscopic study. *Brain Res.* **657**, 31-41.
- Kita, H. & Kitai, S.T. (1994) The morphology of globus pallidus projection neurons in the rat: an intracellular staining study. *Brain Res.* **636**, 308-319.
- Klausberger, T., Roberts, J.D., Somogyi, P. (2002) Cell type- and input-specific differences in the number and subtypes of synaptic GABA(A) receptors in the hippocampus. *J. Neurosci.* **22**, 2513-2521.
- Kneussel, M., Brandstätter, J.H., Gasnier, B., Feng, G., Sanes, J.R., Betz, H. (2001) Gephyrin-independent clustering of postsynaptic GABA(A) receptor subtypes. *Mol. Cell. Neurosci.* **6**, 973-82.
- Kuhn, A.A., Kupsch, A., Schneider, G.H., Brown, P. (2006) Reduction in subthalamic 8-35 Hz oscillatory activity correlates with clinical improvement in Parkinson's disease. *Eur. J. Neurosci.* **23**, 1956-1960.
- Langer, S.Z F-hC, Seeburg, P., Graham, D., Arbilla, S. (1992) The selectivity of zolpidem and alpidem for the alpha1-subunit of the GABAA receptor. *Eur. Neuropsychopharmacol.* **2**, 232-234.
- Lavoie, A.M., Tingey, J.J., Harrison, N.L., Pritchett, D.B., Twyman, R.E. (1997) Activation and deactivation rates of recombinant GABA(A) receptor channels are dependent on alpha-subunit isoform. *Biophys. J.* **73**, 2518-2526.
- Lévi, S., Logan, S.M., Tovar, K.R., Craig, A.M. (2004) Gephyrin is critical for glycine receptor clustering but not for the formation of functional GABAergic synapses in hippocampal neurons. *J. Neurosci.* **24**, 207-17.
- Levitan, E.S., Blair, L.A., Dionne, V.E., Barnard, E.A. (1988) Biophysical and pharmacological properties of cloned GABAA receptor subunits expressed in *Xenopus* oocytes. *Neuron* **1**, 773-781.
- Levy, R., Hutchison, W.D., Lozano, A.M., Dostrovsky, J.O. (2000) High-frequency synchronization of neuronal activity in the subthalamic nucleus of parkinsonian patients with limb tremor. *J. Neurosci.* **20**, 7766-7775.
- Mann, E.O., Paulsen, O. (2007) Role of GABAergic inhibition in hippocampal network oscillations. *Trends Neurosci.* **30**, 343-349.

McKernan, R.M., Rosahl, T.W., Reynolds, D.S., Sur, C., Wafford, K.A., Atack, J.R., Farrar, S., Myers, J., Cook, G., Ferris, P., Garrett, L., Bristow, L., Marshall, G., Macaulay, A., Brown, N., Howell, O., Moore, K.W., Carling, R.W., Street, L.J., Castro, J.L., Ragan, C.I., Dawson, G.R., Whiting, P.J. (2000) Sedative but not anxiolytic properties of benzodiazepines are mediated by the GABA(A) receptor alpha1 subtype. *Nat. Neurosci.* **3**, 87-92.

Miles, R., Toth, K., Gulyas, A.I., Hajos, N., Freund, T.F. (1996) Differences between somatic and dendritic inhibition in the hippocampus. *Neuron* **16**, 815-823.

Nambu, A. & Llinas, R. (1994) Electrophysiology of globus pallidus neurons in vitro. *J. Neurophysiol.* **72**, 1127-1139.

Newell, J.G. & Dunn, S.M. (2002) Functional consequences of the loss of high affinity agonist binding to gamma-aminobutyric acid type A receptors. Implications for receptor desensitization. *J. Biol. Chem.* **277**, 21423-21430.

Nusser, Z., Sieghart, W., Somogyi, P. (1998) Segregation of different GABAA receptors to synaptic and extrasynaptic membranes of cerebellar granule cells. *J. Neurosci.* **18**, 1693-1703.

Nyiri, G., Freund, T.F., Somogyi, P. (2001) Input-dependent synaptic targeting of alpha(2)-subunit-containing GABA(A) receptors in synapses of hippocampal pyramidal cells of the rat. *Eur. J. Neurosci.* **13**, 428-442.

Okoyama, S., Nakamura, Y., Moriizumi, T., Kitao, Y. (1987) Electron microscopic analysis of the synaptic organization of the globus pallidus in the cat. *J. Comp. Neurol.* **265**, 323-331.

Parent, A. & Hazrati, L.N. (1995) Functional anatomy of the basal ganglia. II. The place of subthalamic nucleus and external pallidum in basal ganglia circuitry. *Brain Res. Rev.* **20**, 128-154.

Pirker, S., Schwarzer, C., Wieselthaler, A., Sieghart, W., Sperk, G. (2000) GABA(A) receptors: immunocytochemical distribution of 13 subunits in the adult rat brain. *Neuroscience* **101**, 815-850.

Pritchett, D.B. & Seeburg, P.H. (1990) Gamma-aminobutyric acidA receptor alpha 5-subunit creates novel type II benzodiazepine receptor pharmacology. *J. Neurochem.* **54**, 1802-1804.

Ramerstorfer J., Furtmüller R., Vogel E., Huck S., Sieghart W. (2010) The point mutation gamma 2F77I changes the potency and efficacy of benzodiazepine site ligands in different GABAA receptor subtypes. *Eur. J. Pharmacol.* **636**, 18-27.

Ramming, M., Kins, S., Werner, N., Hermann, A., Betz, H., Kirsch, J. (2000) Diversity and phylogeny of gephyrin: tissue-specific splice variants, gene structure, and sequence similarities to molybdenum cofactor-synthesizing and cytoskeleton-associated proteins. *Proc. Natl. Acad. Sci. USA* **97**, 10266-10271.

Rav-Acha, M., Sagiv, N., Segev, I., Bergman, H., Yarom, Y. (2005) Dynamic and spatial features of the inhibitory pallidal GABAergic synapses. *Neuroscience* **135**, 791-802.

- Sadek, A.R., Magill, P.J., Bolam, J.P. (2007) A single-cell analysis of intrinsic connectivity in the rat globus pallidus. *J. Neurosci.* **27**, 6352-6362.
- Sato, F., Lavallee, P., Levesque, M., Parent, A. (2000) Single-axon tracing study of neurons of the external segment of the globus pallidus in primate. *J. Comp. Neurol.* **417**, 17-31.
- Schneider Gasser, E.M., Straub, C.J., Panzanelli, P., Weinmann, O., Sassoe-Pognetto, M., Fritschy, JM. (2006) Immunofluorescence in brain sections: simultaneous detection of presynaptic and postsynaptic proteins in identified neurons. *Nat. Protoc.* **1**, 1887-1897.
- Schwarzer, C., Berresheim, U., Pirker, S., Wieselthaler, A., Fuchs, K., Sieghart, W., Sperk, G. (2001) Distribution of the major gamma-aminobutyric acid(A) receptor subunits in the basal ganglia and associated limbic brain areas of the adult rat. *J. Comp. Neurol.* **433**, 526-549.
- Semyanov, A., Walker, M.C., Kullmann, D.M. (2003) GABA uptake regulates cortical excitability via cell type-specific tonic inhibition. *Nat. Neurosci.* **6**, 484-490.
- Shink, E., Bevan, M.D., Bolam, JP., Smith, Y. (1996) The subthalamic nucleus and the external pallidum: two tightly interconnected structures that control the output of the basal ganglia in the monkey. *Neuroscience* **73**, 335-357.
- Sieghart, W. (1995) Structure and pharmacology of gamma-aminobutyric acidA receptor subtypes. *Pharmacol. Rev.* **47**, 181-234.
- Sigel, E. (2002) Mapping of the benzodiazepine recognition site on GABA(A) receptors. *Curr. Top. Med. Chem.* **2**, 833-839.
- Sims, R.E., Woodhall, G.L., Wilson, C.L., Stanford, I.M. (2008) Functional characterization of GABAergic pallidopallidal and striatopallidal synapses in the rat globus pallidus in vitro. *Eur. J. Neurosci.* **28**, 2401-2408.
- Smith, Y. & Bolam, JP. (1989) Neurons of the substantia nigra reticulata receive a dense GABA-containing input from the globus pallidus in the rat. *Brain Res.* **493**, 160-167.
- Smith, Y., Bolam, JP., Von Krosigk, M. (1990) Topographical and synaptic organization of the GABA-containing pallidosubthalamic projection in the rat. *Eur. J. Neurosci.* **2**, 500-511.
- Stanford, I.M. (2003) Independent neuronal oscillators of the rat globus pallidus. *J. Neurophysiol.* **89**, 1713-1717.
- Traub, R.D., Whittington, M.A., Colling, S.B., Buzsaki, G., Jefferys, J.G. (1996) Analysis of gamma rhythms in the rat hippocampus in vitro and in vivo. *J. Physiol.* **493**, 471-484.
- Tretter, V., Ehya, N., Fuchs, K., Sieghart, W. (1997) Stoichiometry and assembly of a recombinant GABAA receptor subtype. *J. Neurosci.* **17**, 2728-2737.
- Voorn, P., van de Witte, S., Tjon, G., Jonker, A.J. (1999) Expression of enkephalin in pallido-striatal neurons. *Ann. N. Y. Acad. Sci.* **877**, 671-5.

Wilson, C.J. & Phelan, K.D. (1982) Dual topographic representation of neostriatum in the globus pallidus of rats. *Brain Res.* **243**, 354-359.

Yamawaki, N., Stanford, I.M., Hall, S.D., Woodhall, G.L. (2008) Pharmacologically induced and stimulus evoked rhythmic neuronal oscillatory activity in the primary motor cortex in vitro. *Neuroscience* **151**, 386-395.

PRIMARY ANTIBODIES against	SPECIES and DILUTIONS	SOURCE and CHARACTERIZATION	SECONDARY ANTIBODIES DILUTION and SOURCE	NUMBER OF SECTIONS / NUMBER OF ANIMALS
GABA_Aα1	Rabbit (1:10000)	(Fritschy and Mohler, 1995)	donkey-α-rb Alexa 488 (1:1000); CY5 (1:250)	10/5
GABA_Aα2	Rabbit (1:1000)	(Kasugai et al., 2010)	donkey-α-rb Alexa 488 (1:1000) Invitrogen, Molecular Probes	5/3
GABA_Aα3	Guinea-pig (1:4000)	(Fritschy and Mohler, 1995)	donkey-α-gp CY3 (1:400) Jackson Laboratories	8/4
GABA_A γ2	Rabbit (1:200)	(Kasugai et al., 2010)	donkey-α-rb Alexa 488 (1:1000) Invitrogen, Molecular Probes	3/3
GABA_A γ2	Guinea-pig (1:250)	(Fritschy and Mohler, 1995)	donkey-α-gp CY3 (1:400) Jackson Laboratories	3/3
gephyrin	Mouse (1:1000)	Synaptic Systems #mAB7a (Jacob et al., 2005) (Schneider Gasser et al., 2006)	donkey-α-m CY3 (1:400) Jackson Laboratories	10/5
parvalbumin	Guinea-pig (1:1000)	Synaptic Systems #195 004	donkey-α-gp CY5 (1:250) Jackson Laboratories	5/3
enkephalin	Mouse (1:500)	Chemicon #MAB 350 (Lindemeyer et al., 2006)	donkey-α-m CY3 (1:400) Jackson Laboratories	5/3
HuC/D	Mouse (1:100)	Molecular Probes #A-21271 (Fornaro and Geuna, 2005)	donkey-α-m CY5 (1:250) Jackson Laboratories	3/3

VGAT	Guinea-pig (1:500)	Synaptic Systems #131 005 (Gronborg et al., 2010)	CY5 (1:250) Jackson Laboratories	4/2
-------------	-----------------------	---	--	-----

Table 1. Details of primary and secondary antibodies

	primary antibodies (dilution)	secondary antibodies (dilution)
experiment # 1		
	GABA _A α1 (rb) (1:10000)	donkey α-rb-488 (1:1000)
	gephyrin (m) (1:1000)	donkey α-m-CY3 (1:400)
	PV (gp) (1:1000)	donkey α-gp-CY5 (1:250)
CONTROL		
	x	donkey α-rb-488 (1:1000)
	x	donkey α-m-CY3 (1:400)
	x	donkey α-gp-CY5 (1:250)
	GABA _A α1 (rb) 1:10000	donkey α-m-CY3 (1:400)
	x	donkey α-gp-CY5 (1:250)
	gephyrin (m) 1:1000	donkey α-rb-488 (1:1000)
	x	donkey α-gp-CY5 (1:250)
	PV (gp) 1:1000	donkey α-rb-488 (1:1000)
	x	donkey α-m-CY3 (1:400)
experiment # 2		
	GABA _A α1 (rb) (1:10000)	donkey α-rb-488 (1:1000)
	Enk (m) (1:500)	donkey α-m-CY3 (1:400)
	PV (gp) (1:1000)	donkey α-gp-CY5 (1:250)
CONTROL		
	Enk (m) (1:500)	donkey α-rb-488 (1:1000)
	x	donkey α-gp-CY5 (1:250)
experiment # 3		
	GABA _A α1 (rb) (1:10000)	donkey α-rb-488 (1:1000)
	GABA _A γ2 (gp) (1:250)	donkey α-gp-CY3 (1:400)
CONTROL		
	x	donkey α-gp-CY3 (1:400)
	GABA _A α1 (rb) (1:10000)	donkey α-gp-CY3 (1:400)
	GABA _A γ2 (gp) (1:250)	donkey α-rb-488 (1:1000)
experiment # 4		
	GABA _A α1 (rb) (1:10000)	donkey α-rb-488 (1:1000)
	GABA _A α3 (gp) (1:4000)	donkey α-gp-CY3 (1:400)
	HuCD (m) (1:100)	donkey α-m-CY5 (1:250)
CONTROL		
	x	donkey α-gp-CY3 (1:400)
	x	donkey α-m-CY5 (1:250)
	GABA _A α1 (rb) (1:10000)	donkey α-gp-CY3 (1:400)
	x	donkey α-m-CY5 (1:250)
	GABA _A α3 (gp) (1:4000)	donkey α-rb-488 (1:1000)
	x	donkey α-m-CY5 (1:250)
	HuCD (m) (1:100)	donkey α-rb-488 (1:1000)

experiment # 5		
	GABA _A α3 (gp) 1:4000	goat α-gp-488 (1:1000)
	gephyrin (m) 1:1000	donkey α-m-CY3 (1:400)
CONTROL		
	x	goat α-gp-488 (1:1000)
	GABA _A α3 (gp) 1:4000	donkey α-m-CY3 (1:400)
	gephyrin (m) 1:1000	goat α-gp-488 (1:1000)
experiment # 6		
	GABA _A α3 (gp) 1:4000	donkey α-gp-488 (1:1000)
	Enk (m) 1:500	donkey α-m-CY3 (1:400)
	PV(rb) 1:1000	donkey α-rb-CY5 (1:250)
CONTROL		
	x	donkey α-rb-CY5 (1:250)
	GABA _A α3 (gp) 1:4000	donkey α-rb-CY5 (1:250)
		donkey α-m-CY3 (1:400)
	Enk (m) 1:500	donkey α-gp-488 (1:1000)
		donkey α-rb-CY5 (1:250)
	PV(rb) 1:1000	donkey α-gp-488 (1:1000)
		donkey α-m-CY3 (1:400)
experiment # 7		
	GABA _A α2 (rb) (1:10000)	donkey α-rb-488 (1:1000)
	gephyrin (m) 1:1000	donkey α-m-CY3 (1:400)
	PV(gp) 1:1000	donkey α-gp-488 (1:1000)
CONTROL		
	GABA _A α2 (rb) (1:10000)	donkey α-m-CY3 (1:400)
		donkey α-gp-488 (1:1000)
experiment # 8		
	GABA _A α2 (rb) (1:10000)	donkey α-rb-488 (1:1000)
	GABA _A γ2 (gp) (1:250)	donkey α-gp-CY3 (1:400)
CONTROL		
	GABA _A α2 (rb) (1:10000)	donkey α-gp-CY3 (1:400)
experiment # 9		
	GABA _A α3 (gp) 1:4000	donkey α-gp-488 (1:1000)
	GABA _A γ2 (rb) (1:250)	donkey α-rb-CY3 (1:400)
CONTROL		
	x	donkey α-rb-CY3 (1:400)
	GABA _A α3 (gp) 1:4000	donkey α-rb-CY3 (1:400)
	GABA _A γ2 (rb) (1:250)	donkey α-gp-488 (1:1000)

Supplementary table 1 : Control experiments

abbreviations: (m: mouse; rb: rabbit; gp: guinea pig)

FIGURE LEGENDS

Figure 1. The $\alpha 1$ subunit is widely distributed in GP and is present at both Str-GP and GP-GP synapses.

(A) Diazepam (500 nM) was added after 10 min baseline recording. At both Str-GP (n=6, black) and GP-GP (n=6, red) synapses the IPSC amplitude (**A/1 and A/2**) and decay times (**A/3 and A/4**) were significantly increased. Each point represents the average of six responses. Data traces (once again average of six) are shown for baseline (dark) and after 15 min diazepam (light) for both Str-GP (**A/5**) and GP-GP (**A/6**) synapses. **(B)** 100 nM zolpidem (selective for $\alpha 1$ GABA_A subunits) was added 10 min after baseline recording. At both Str-GP (n=6, black) and GP-GP (n=6, red) synapses the IPSC amplitude (**B/1 and B/2**) and decay times (**B/3 and B/4**) were significantly increased. Data traces (average of six) are shown for baseline (dark) and after 15 min zolpidem (light) for both Str-GP (**B/5**) and GP-GP (**B/6**) synapses.

Figure 2. GABA_A $\alpha 1$ subunit immunoreactivity in globus pallidus neurons

(A): Low magnification confocal image showing strong immunoreactivity for the GABA_A $\alpha 1$ subunit in GP and weak immunoreactivity in striatum. **(B-E)**: Triple immunofluorescent labeling for the $\alpha 1$ subunit (green, **B**), gephyrin (red, **C**) and parvalbumin (blue, **D**). **(B)**: GABA_A $\alpha 1$ subunit immunoreactivity is widely distributed in the somata (arrows) and dendrites (arrowhead) of GP neurons. **(C)**: GP neurons exhibit either strong (arrows) or weak (asterisk) gephyrin immunoreactivity. **(D)**: Confocal image illustrating parvalbumin-positive (arrows) and negative neurons (asterisk) in GP. **(E)**: Merged image showing that some GABA_A $\alpha 1$ subunit-positive but parvalbumin-negative GP neurons (asterisk) show strikingly weak immunoreactivity for gephyrin, whereas other neurons (arrows) and dendrites (arrowhead) are immunoreactive for all three markers. Scale in E also applies to B, C and D **(F)**: Bar charts of the proportions of GP neurons expressing GABA_A $\alpha 1$ subunit immunoreactivity (green) and the proportion of these that show strong (red) and weak (pink) immunoreactivity for gephyrin. **(G-J)**: Triple immunofluorescent labeling showing GABA_A $\alpha 1$ subunit- and parvalbumin-positive neurons closely apposed by enkephalin-positive striatal axon terminals. **(H)**: Confocal image illustrating very dense enkephalin immunoreactivity in GP associated with somata (arrow) and dendrites (arrowhead). **(I)**: The same somata and dendrite as in H are immunopositive for parvalbumin. **(J)**: Merged image showing GABA_A $\alpha 1$ subunit and parvalbumin-positive cell bodies and dendrites closely apposed by many enkephalin-positive striatal axon terminals. Scale in G also applies to H, I and J. **(J/1-J/4)**: High magnification confocal images of the dendrite fragment indicated by an arrowhead in **G-H** showing the co-occurrence of GABA_A $\alpha 1$ subunit immunoreactivity with pre-synaptic enkephalin-immunoreactivity (arrowheads on J/4). Scale in J/4 applies to all four images. **(K-M)**: Confocal images of GP neurons expressing immunoreactivity for the GABA_A $\alpha 1$ subunit co-localized with the GABA_A $\gamma 2$ subunit on somata (double arrowheads) and dendrites (arrowheads). Scale in M also applies to K and L.

Figure 3. A greater number of non- α subunits at GP-GP synapses.

(A) 400nM zolpidem was applied after 10 min baseline recording in 100nM zolpidem. IPSC amplitude (**A/1 and A/2**) and decay times (**A/3 and A/4**) were significantly increased at GP-GP (n=8, red) but not Str-GP (n=8, black) synapses. **(B)** L-838,417 (500nM) was added 10 min after baseline recording. Once again, IPSC amplitude (**B/1 and B/2**) and decay times (**B/3 and B/4**) were significantly increased at GP-GP (n=7, red) but not Str-GP (n=6, black) synapses.

Figure 4 GABA_A α2 subunits are preferentially located in synapses targeting the dendrites of GP neurons.

(A): Low power confocal image showing weak/moderate immunoreactivity for the GABA_A α2 subunit in GP and strong labeling in striatum. **(B-E):** In GP, triple immunofluorescent images illustrating immunoreactivity for the GABA_A α2 subunit (green) and gephyrin (red) in a parvalbumin-expressing (blue) GP neuron. **(B):** Confocal image showing strong, mainly intracellular immunoreactivity for the α2 subunit in the soma (arrow), and punctate labeling in dendrites (arrowheads) of GP neurons. **(C):** Fluorescent image illustrating gephyrin immunoreactivity in somatic (arrow) and dendritic (arrowheads) compartments. **(E):** Merged image illustrating immunoreactivity for the GABA_A α2 subunit (green) and gephyrin (red) in parvalbumin-expressing (blue) GP neuron somata (arrow) and dendrites (arrowheads). Scale in E also applies to B, C and D. **(E/1-4):** High magnification images of the dendritic segment in the boxed area in E. Note the co-localization of the GABA_A α2 subunit immunoreactivity (green) with gephyrin immunoreactivity (red) (arrowheads in E/4). Scale in E/4 applies to all four images. **(F-H):** High power confocal images illustrating the numerous GABA_A α2 subunit puncta associated with the gephyrin labeling (F, green, arrowheads). Merged image in H. Scale in H also applies to F and G.

Figure 5. Preferential localization of the GABA_A α3 subunit at synapses targeting the soma of GP neurons.

(A): Low power confocal image showing weak immunoreactivity for the GABA_A α3 subunit in the GP and strong labeling in the striatum. **(B-D):** Low power images illustrating the co-localization of the two GABA_A subunits; α1 (C, red) and α3 (B, green) in GP neurons (arrows), identified by the neuronal marker, HuC/D (D, blue). **(B):** Note that GABA_A α3 subunit immunoreactivity (green) is mainly present in the soma of GP neurons (arrows), as opposed to the GABA_A α1 subunit immunoreactivity (red, C) which is distributed uniformly in the somatic and dendritic compartments. Scale in D also applies to B and C. **(E):** High power image of a GP neuron displaying strong immunoreactivity for the GABA_A α3 subunit (green) at the soma (double arrowheads) and weaker labeling towards more distal dendritic compartments. **(F):** Strong gephyrin immunoreactivity (red) at both somatic and dendritic compartments indicating extensive inhibitory input to GP neurons. **(G):** Co-localization (double arrowheads) of the GABA_A α3 subunit immunoreactivity (green) and gephyrin immunoreactivity (red) on the surface and intracellularly. Scale in G also applies to E and F. **(H-K):** A GABA_A α3 subunit immunoreactive (green, H) and parvalbumin-positive (blue, J) GP neuron (arrow) closely apposed by enkephalin-positive boutons (red, I) on both somatic and dendritic compartments. Scale in K also applies to H, I and J. **(L):** Strong GABA_A α3 subunit immunoreactivity (green) concentrated in the soma of a GP neuron (double arrowhead). Note the considerably weaker labeling observed on a nearby dendrite (arrowhead). **(M):** GABA_A γ2 subunit immunoreactivity (red) showing strong labeling at both somatic and dendritic compartments of the same structures as in L. **(N):** Merged image illustrating the co-localization of the GABA_A α3 subunit immunoreactivity (green) and GABA_A γ2 subunit immunoreactivity (red) in the soma (double arrowhead) and the lack of co-localization on a nearby dendrite (arrowhead). Scale in N also applies to L and M.

Figure 6. The GABA_A α3 subunit is preferentially located at GP-GP synapses.

100 nM TP003 was added after 10 min of baseline recording. At Str-GP synapses (n=7, black) TP003 had no effect on both IPSC amplitude (**A/1**) and decay time (**A/3**), while at GP-GP synapses (n=7, red), TP003 significantly increased the IPSC amplitude (**A/2**).

Figure 7. Summary indicating cellular distribution of Str-GP and GP-GP synapses

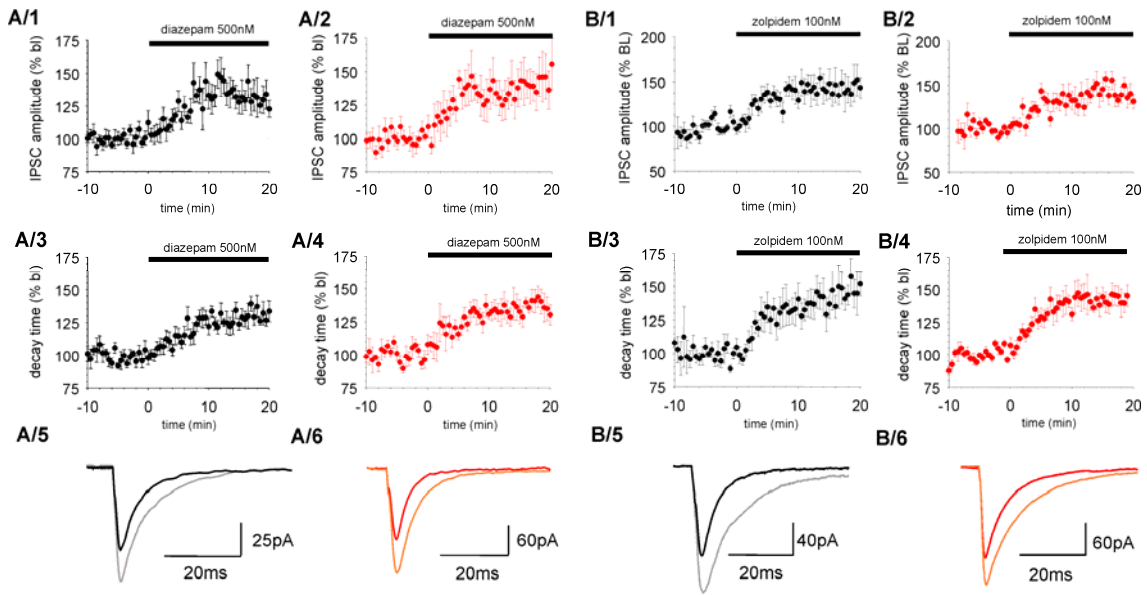
A GP neuron receives its major GABAergic input from striatum (STR terminals-purple) and from neighbouring GP neurons (GP terminals-light green) and glutamatergic input from STN (STN terminals-red) and to a lesser extent, from thalamus. Our results show an even distribution of the GABA_A α1 subunits throughout the soma and dendritic axis of GP neurons. However, there is a differential distribution of the GABA_A α2 and α3 subunits with the α2 preferentially located on the dendrites and α3 preferentially located at the soma where they are targeted by local GP collaterals.

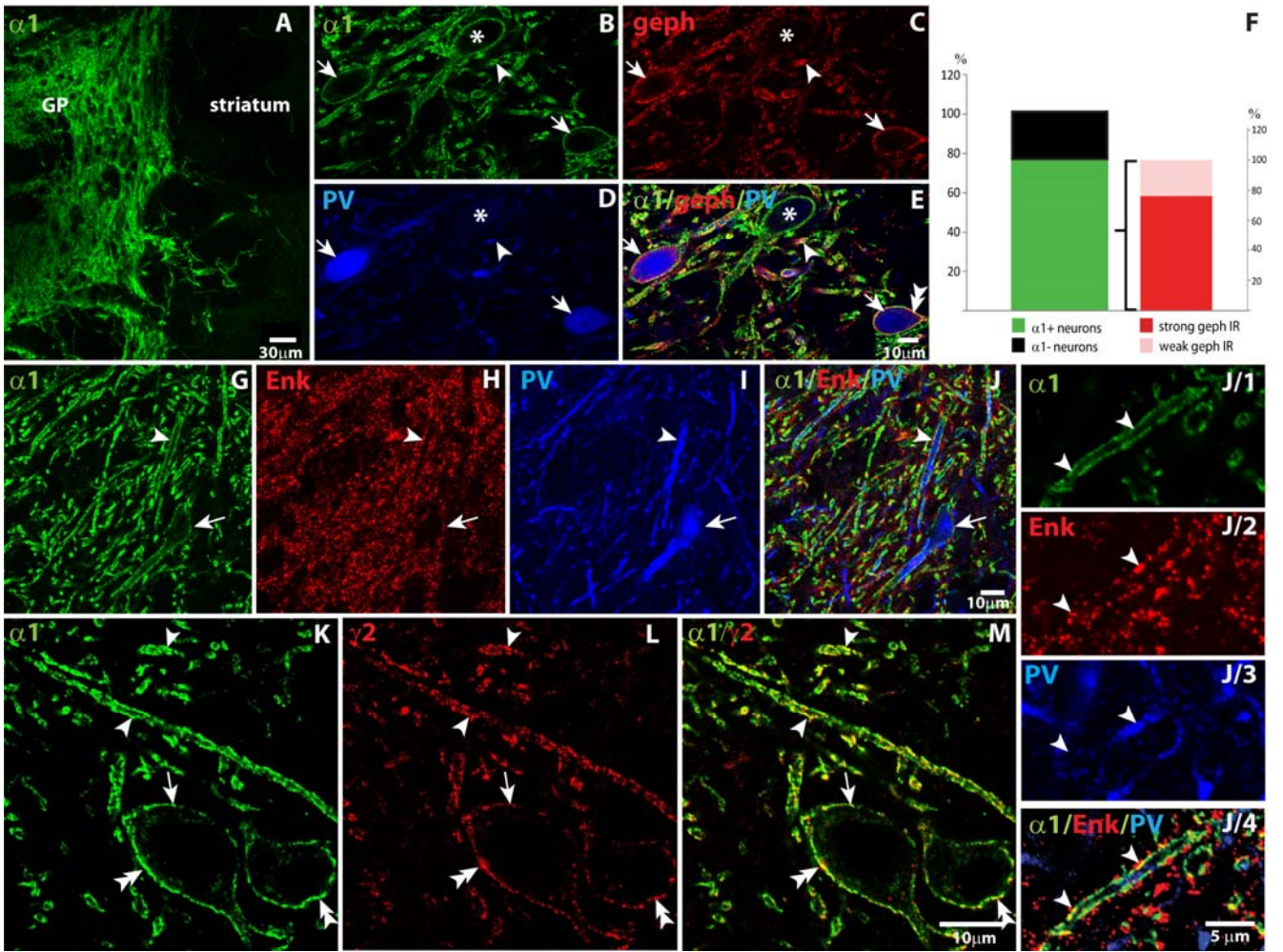
Supplementary Figure 1. GABA_A α1 subunit immunoreactivity in globus pallidus neurons

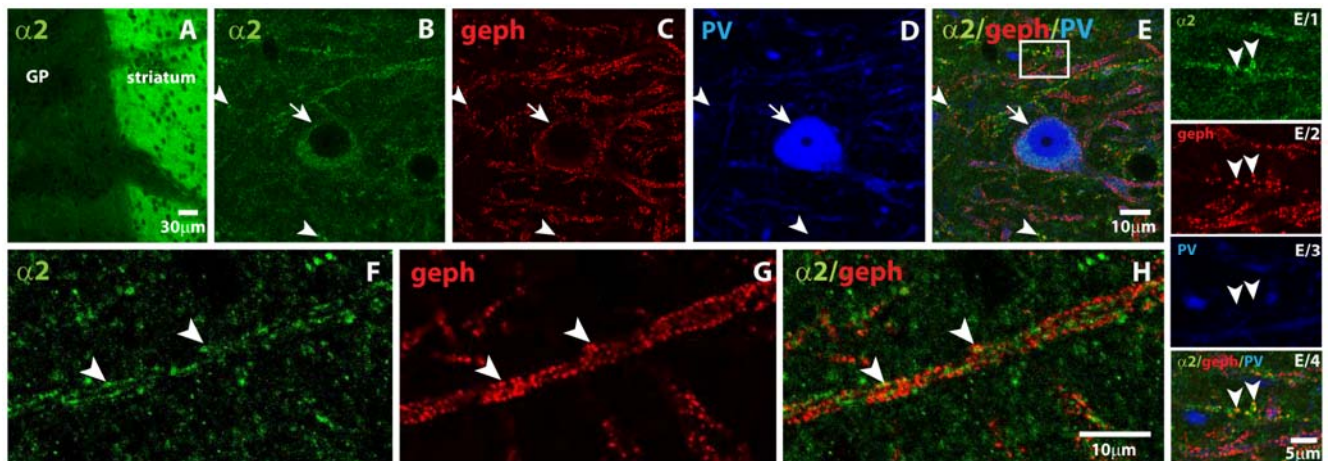
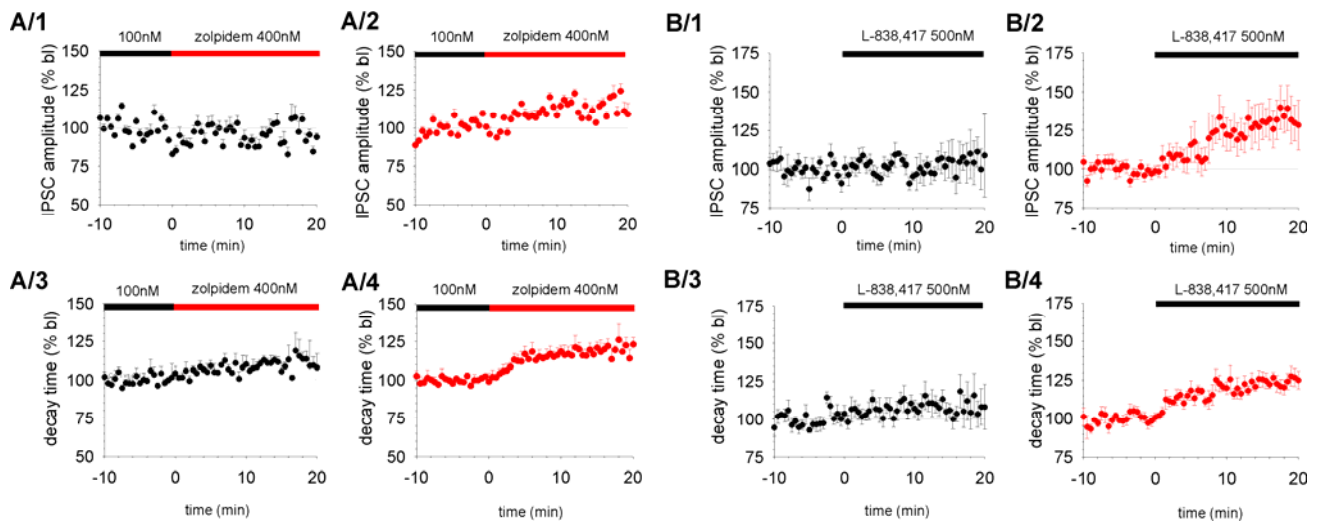
Triple immunofluorescent labeling for the α1 subunit (green, **A**), gephyrin (red, **B**) and VGAT (blue, **C**).

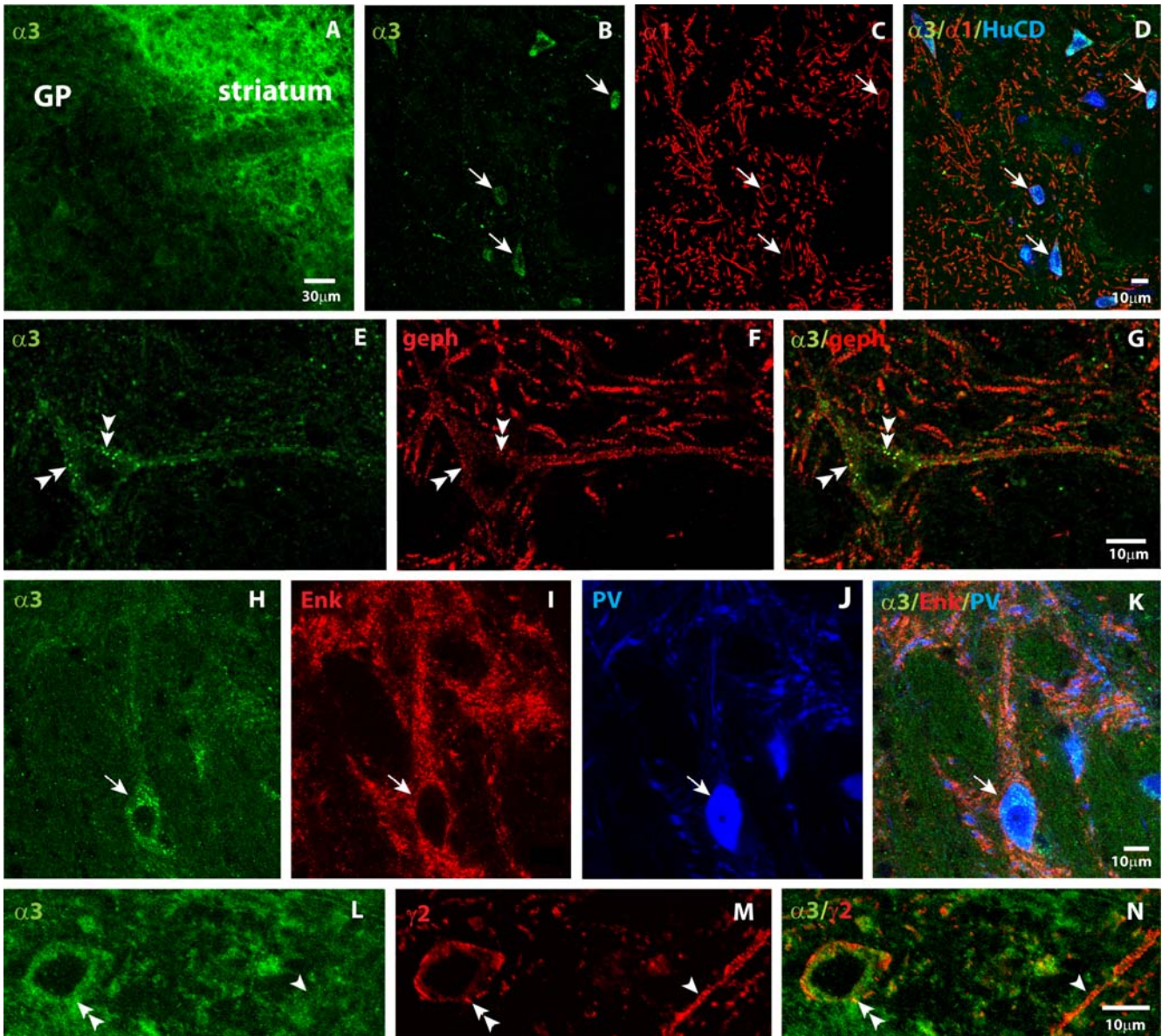
(A): Confocal image showing two GP neurons, both immunopositive for the GABA_Aα1 subunit (arrow, asterisk).

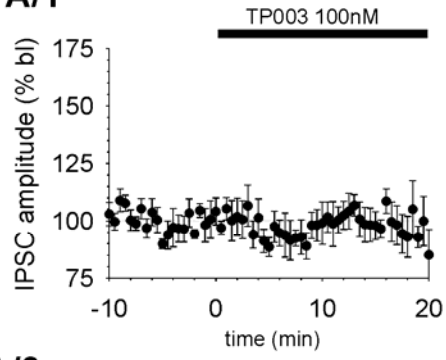
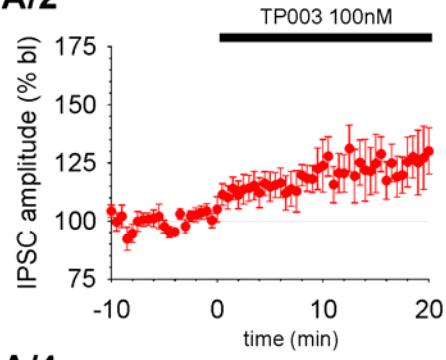
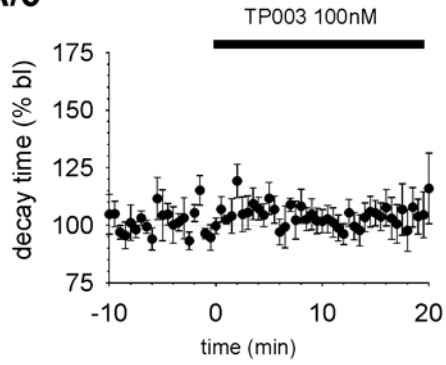
(B): Same GP neurons, expressing different levels of gephyrin immunoreactivity. While one neuron is strongly positive (arrow), the other one shows weak immunoreactivity for gephyrin (asterisk). **(C)**: Confocal image illustrating the immunoreactivity for VGAT in the same GP neurons. **(D)**: Merged image showing the labelling for GABA_Aα1 (green), VGAT (blue) and gephyrin (red). VGAT immunolabeling shows similar distribution to the GABA_A α1 subunit, and unlike gephyrin, no striking difference was observed in the intensity of the immunolabeling in these neurons.









A/1**A/2****A/3****A/4**